Lecture slides as a support of

Advanced Microscopies I: Scanning Tunneling Micrsocopy

Clemens Winkelmann

Master Nanotech / Phelma / Grenoble INP

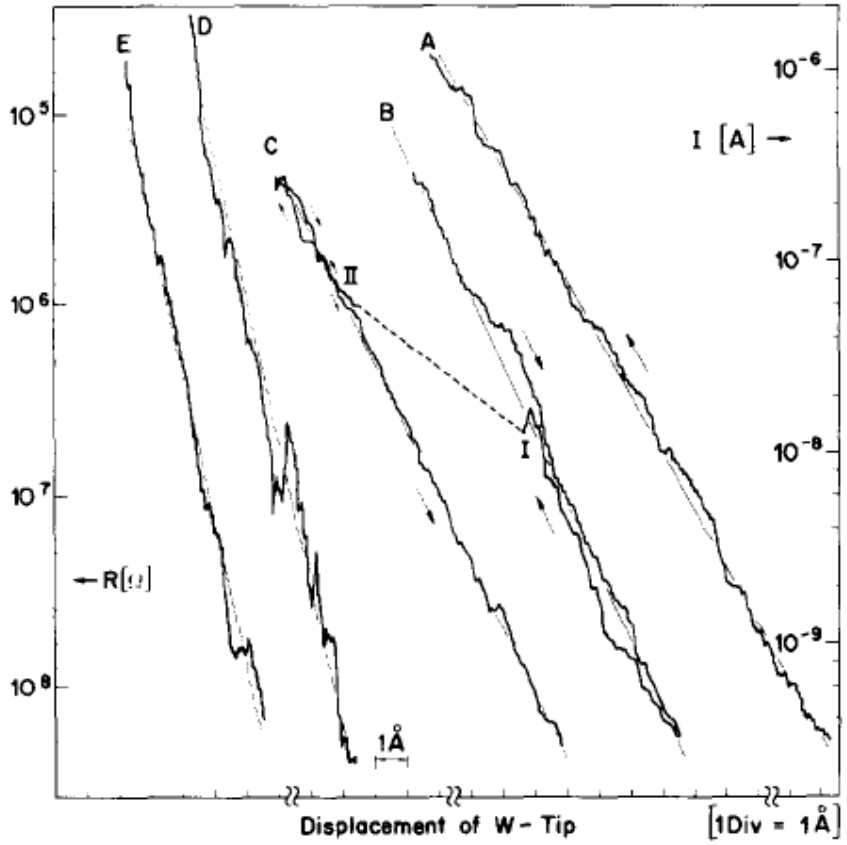

FIG. 2. Tunnel resistance and current vs displacement of Pt plate for different surface conditions as described in the text. The displacement origin is arbitrary for each curve (except for curves B and C with the same origin). The sweep rate was approximately 1 Å/s. Work functions $\phi = 0.6$ eV and 0.7 eV are derived from curves A, B, and C, respectively. The instability which occurred while scanning B and resulted in a jump from point I to II is attributed to the release of thermal stress in the unit. After this, the tunnel unit remained stable within 0.2 Å as shown by curve C. After repeated cleaning and in slightly better vacuum, the steepness of curves D and E resulted in $\phi = 3.2$ eV.

"Tunneling through a controllable vacuum gap", G. Binnig, H. Röhrer, Ch. Gerber and E. Weibel, Appl. Phys. Lett. 40, 178 (1982).

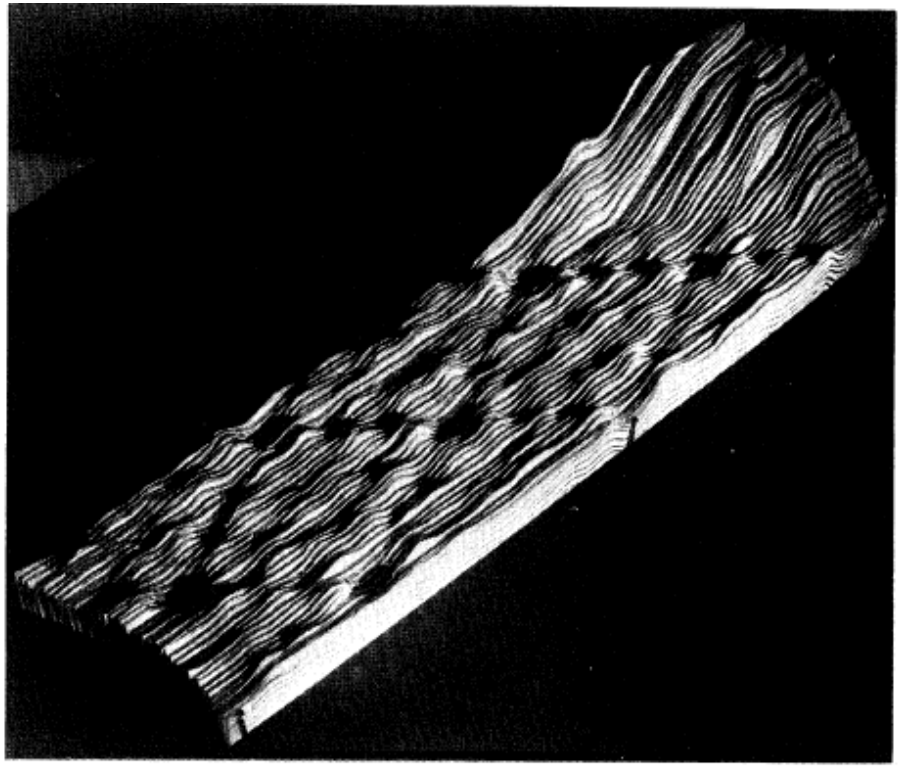

FIG. 1. Relief of two complete 7×7 unit cells, with nine minima and twelve maxima each, taken at 300 °C. Heights are enhanced by 55%; the hill at the right grows to a maximal height of 15 Å. The [$\bar{2}$11] direction points from right to left, along the long diagonal.

"7x7 reconstruction on Si (111) resolved in real space", G. Binnig, H. Röhrer, Ch. Gerber and E. Weibel, Phys. Rev. Lett. 50, 120 (1983).

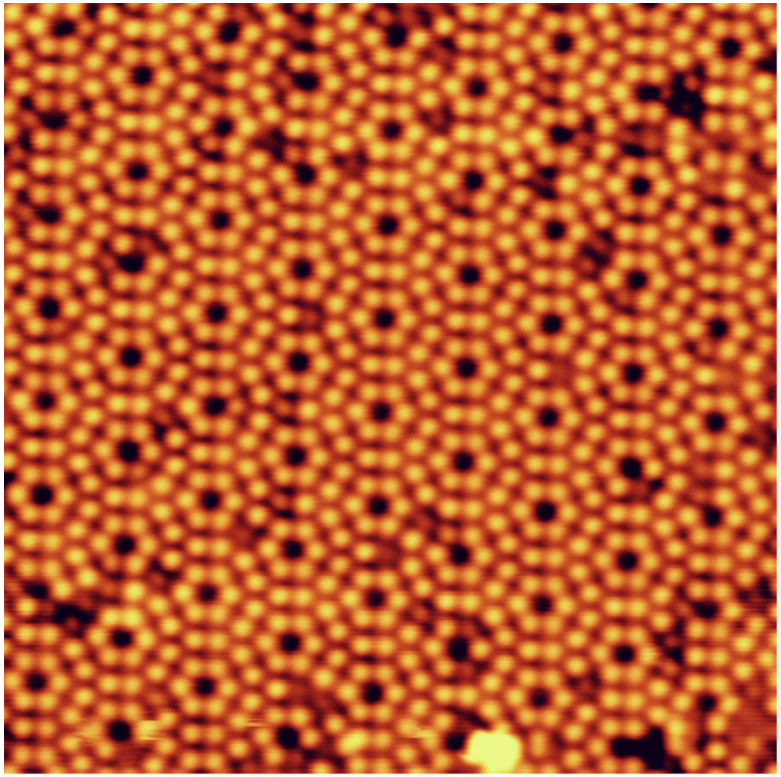

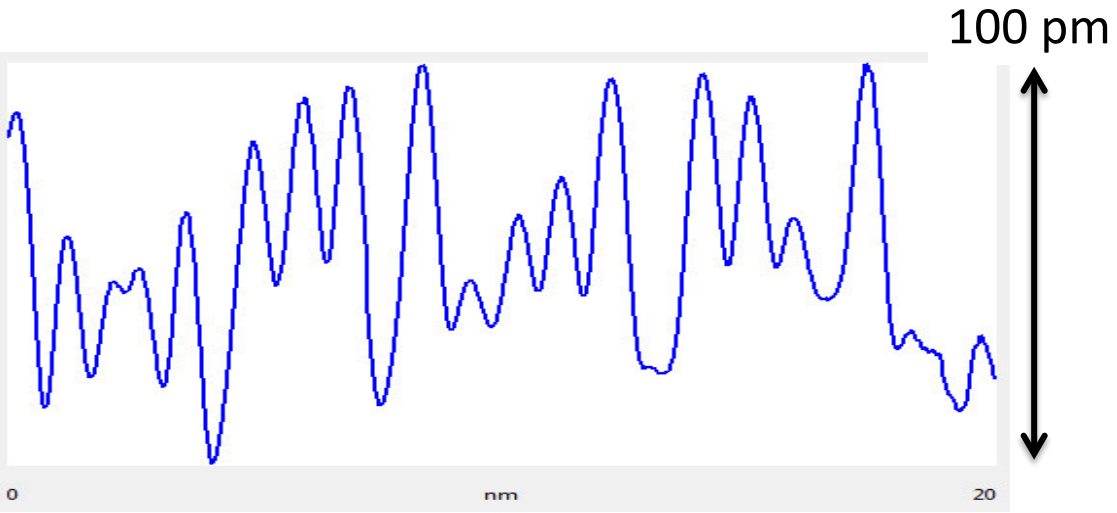

Silicon 7x7 at T = 4.2 K with *Tribus Ultra* Sigma Surface Science

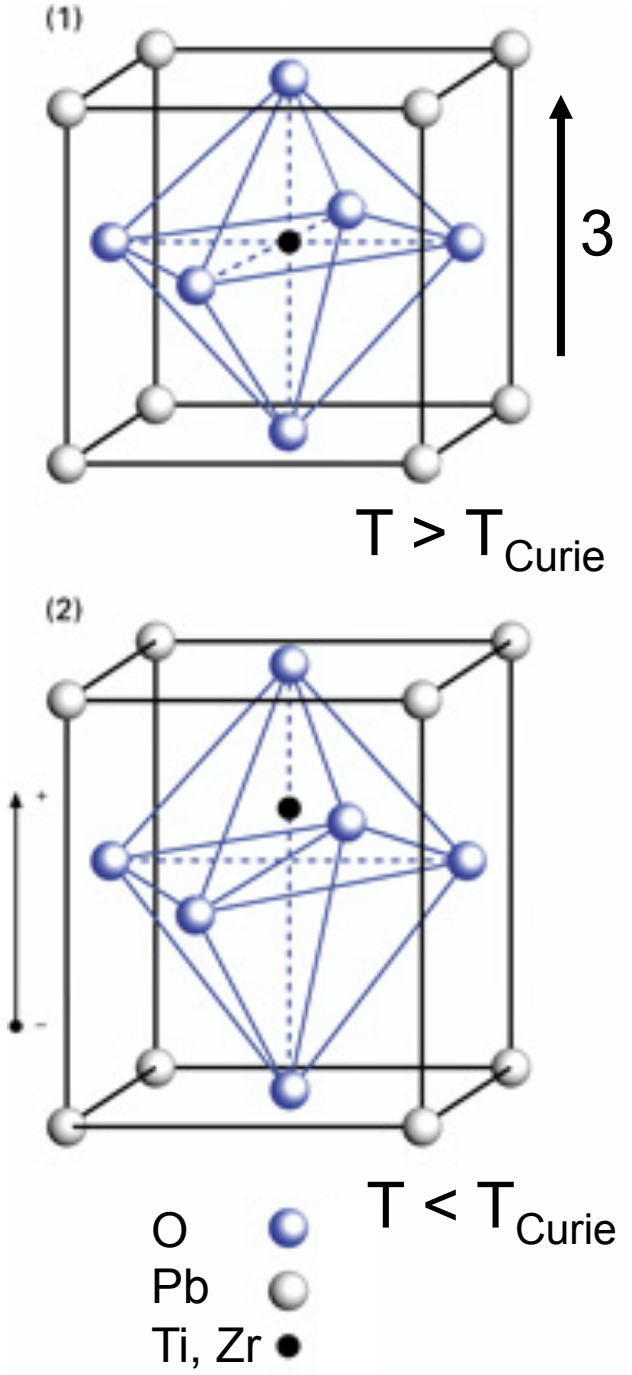
(1)
3
T > T Curie
(2)
+
-
T < T Curie
O
Pb
Ti, Zr

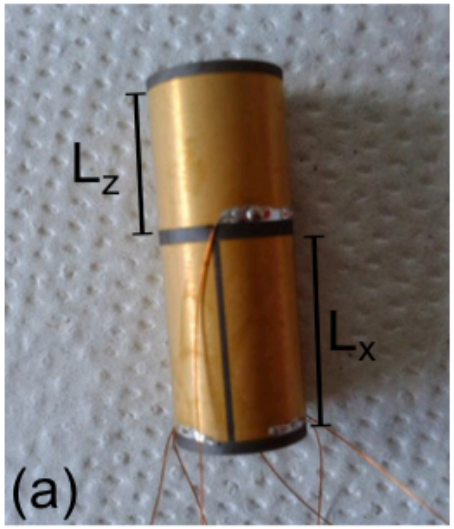
L_z
L_x
(a)

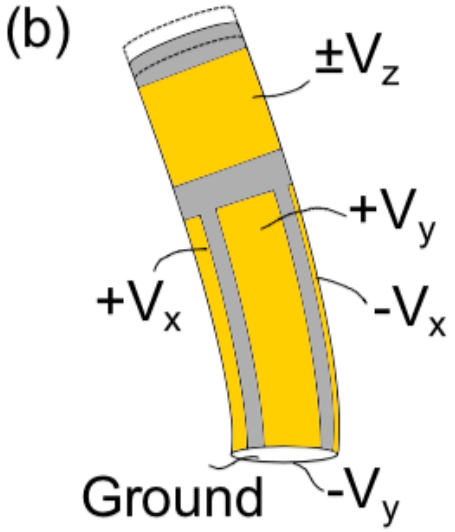
(b)
$\pm V_z$
$+V_y$
$+V_x$
$-V_x$
Ground
$-V_y$

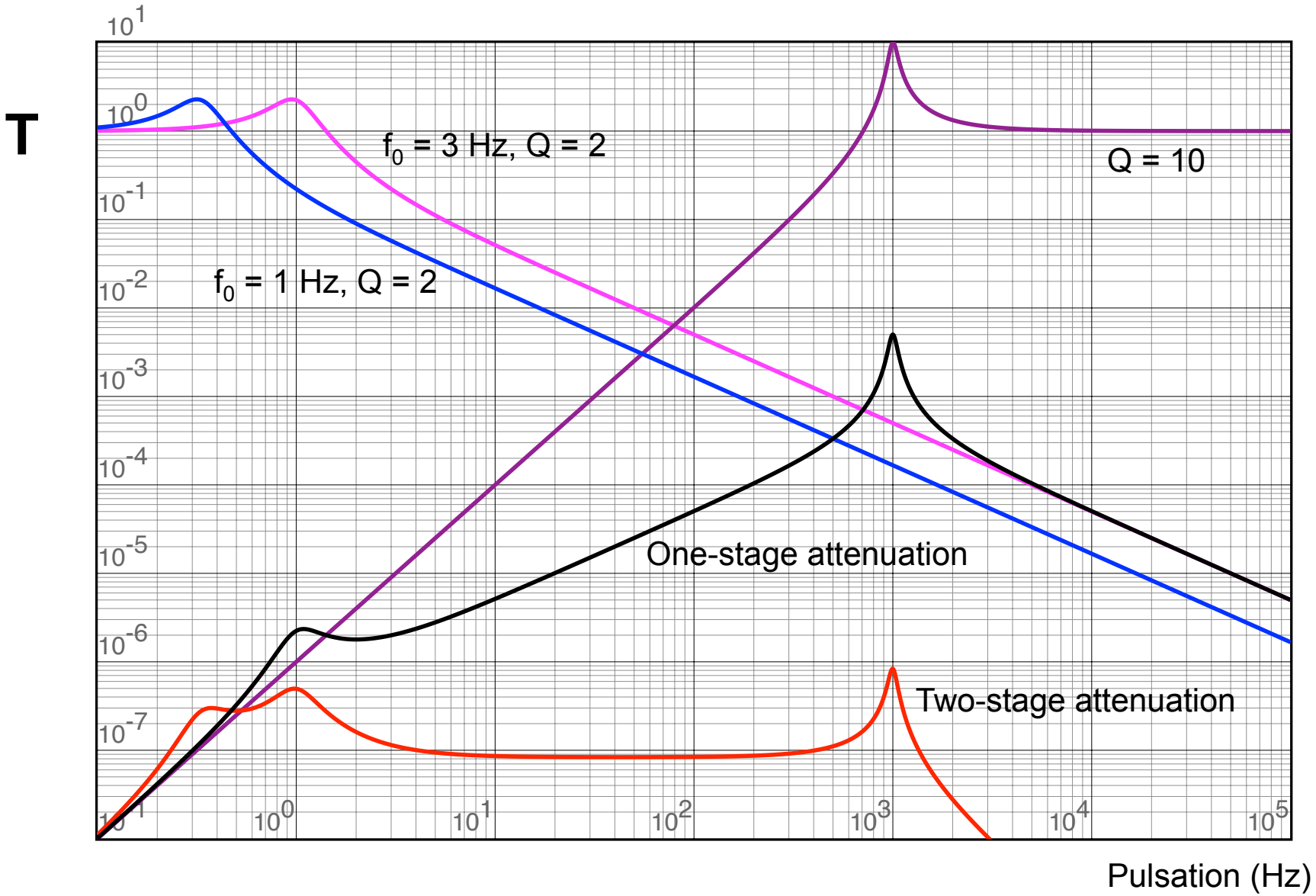
T
10^{1}
10^{0}
10^{-1}
10^{-2}
10^{-3}
10^{-4}
10^{-5}
10^{-6}
10^{-7}
10^{0}
10^{1}
10^{2}
10^{3}
10^{4}
10^{5}
f_0 = 3 Hz, Q = 2
f_0 = 1 Hz, Q = 2
Q = 10
One-stage attenuation
Two-stage attenuation
Pulsation (Hz)

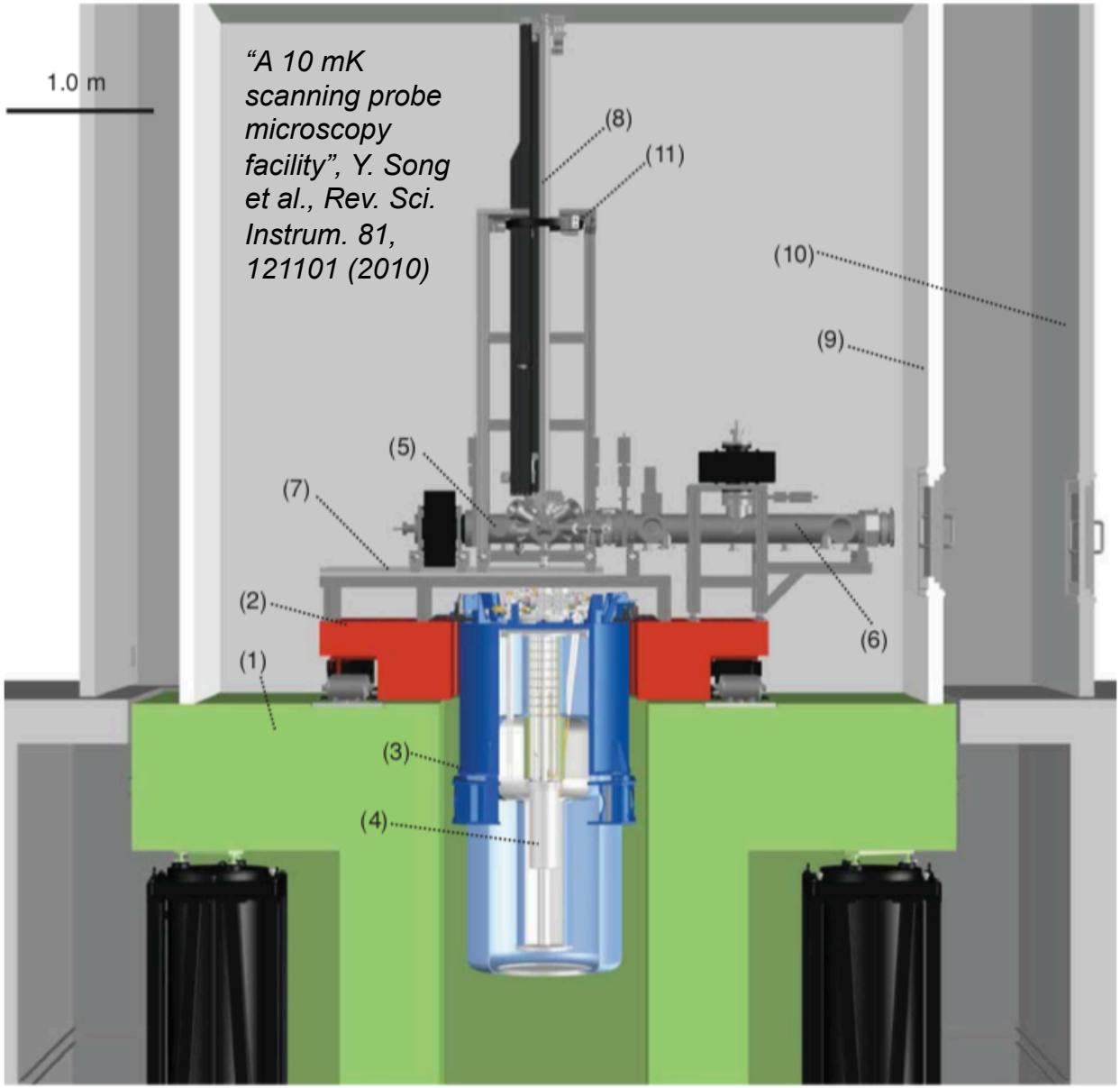

"A 10 mK scanning probe microscopy facility", Y. Song et al., Rev. Sci. Instrum. 81, 121101 (2010)

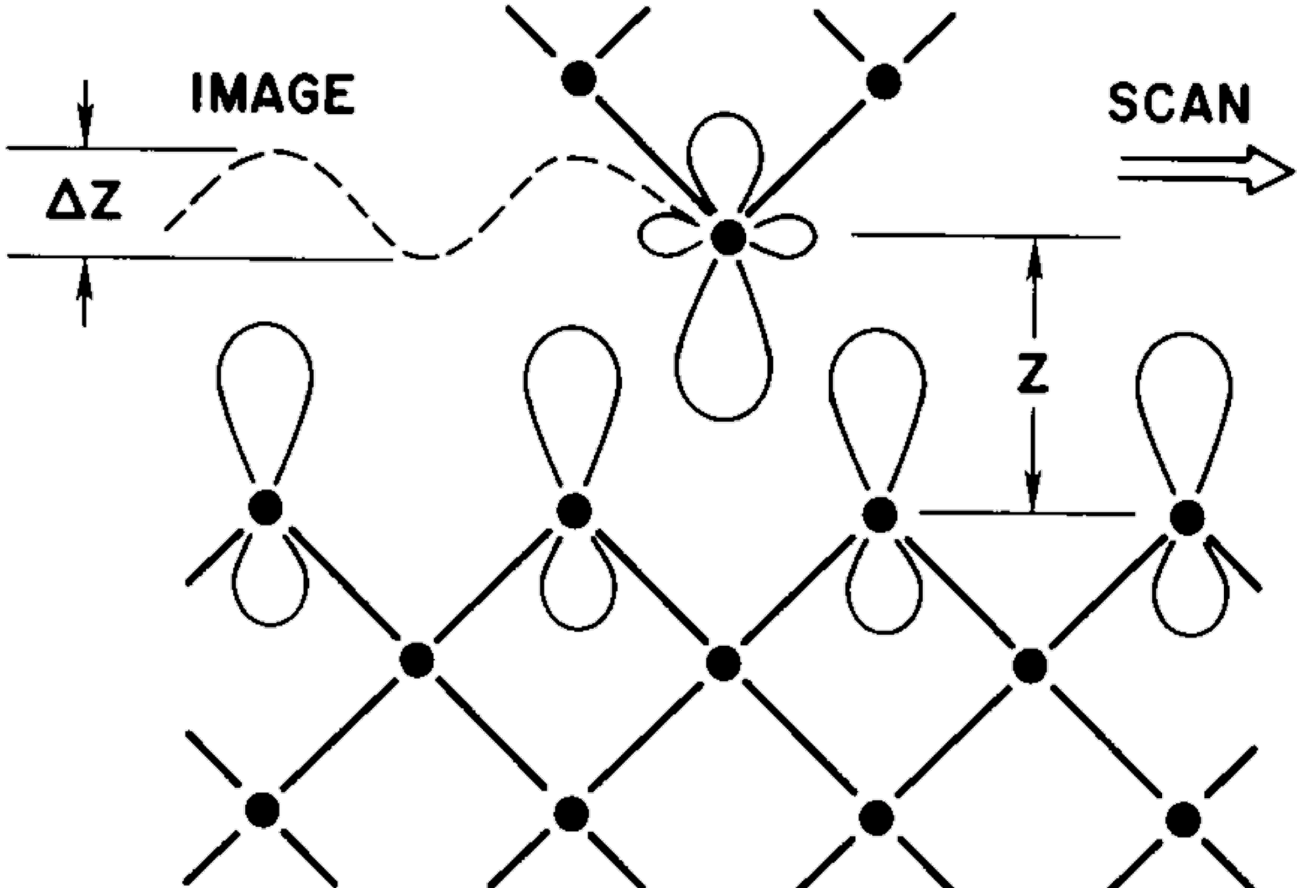
IMAGE
ΔZ
SCAN
Z

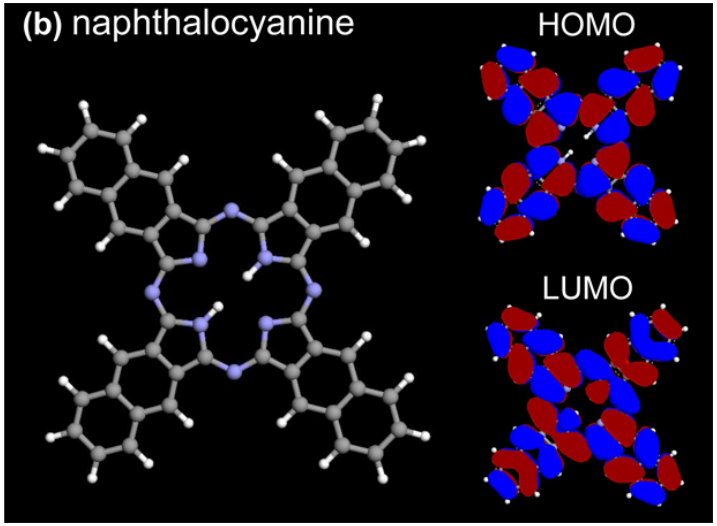

Cu tip: s states
Cu tip with a CO molecule adsorbed: p or s+p states

Contrast enhanced and modified with a CO tip.

L. Gross et al, Phys. Rev. Lett. 107, 086101 (2011).

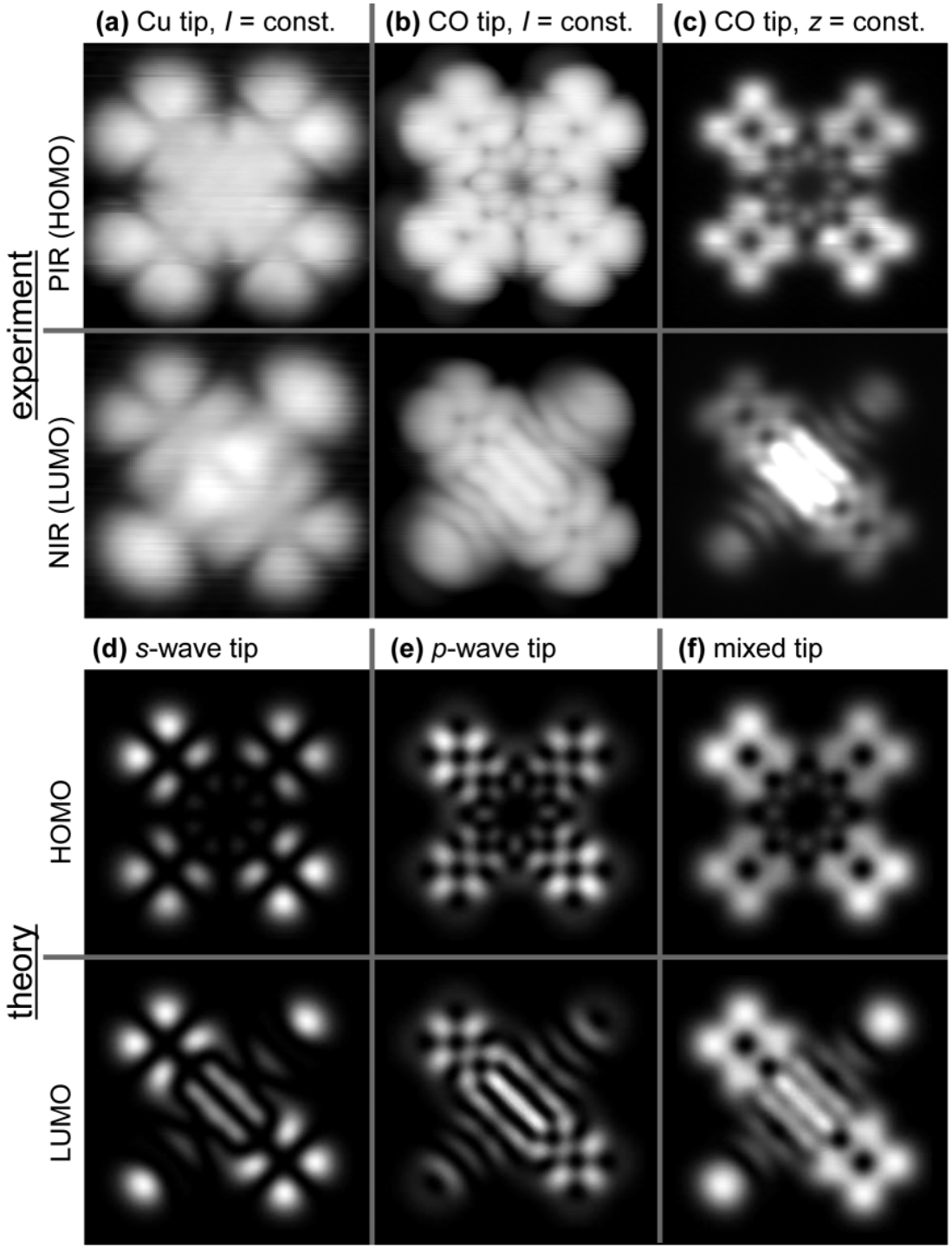

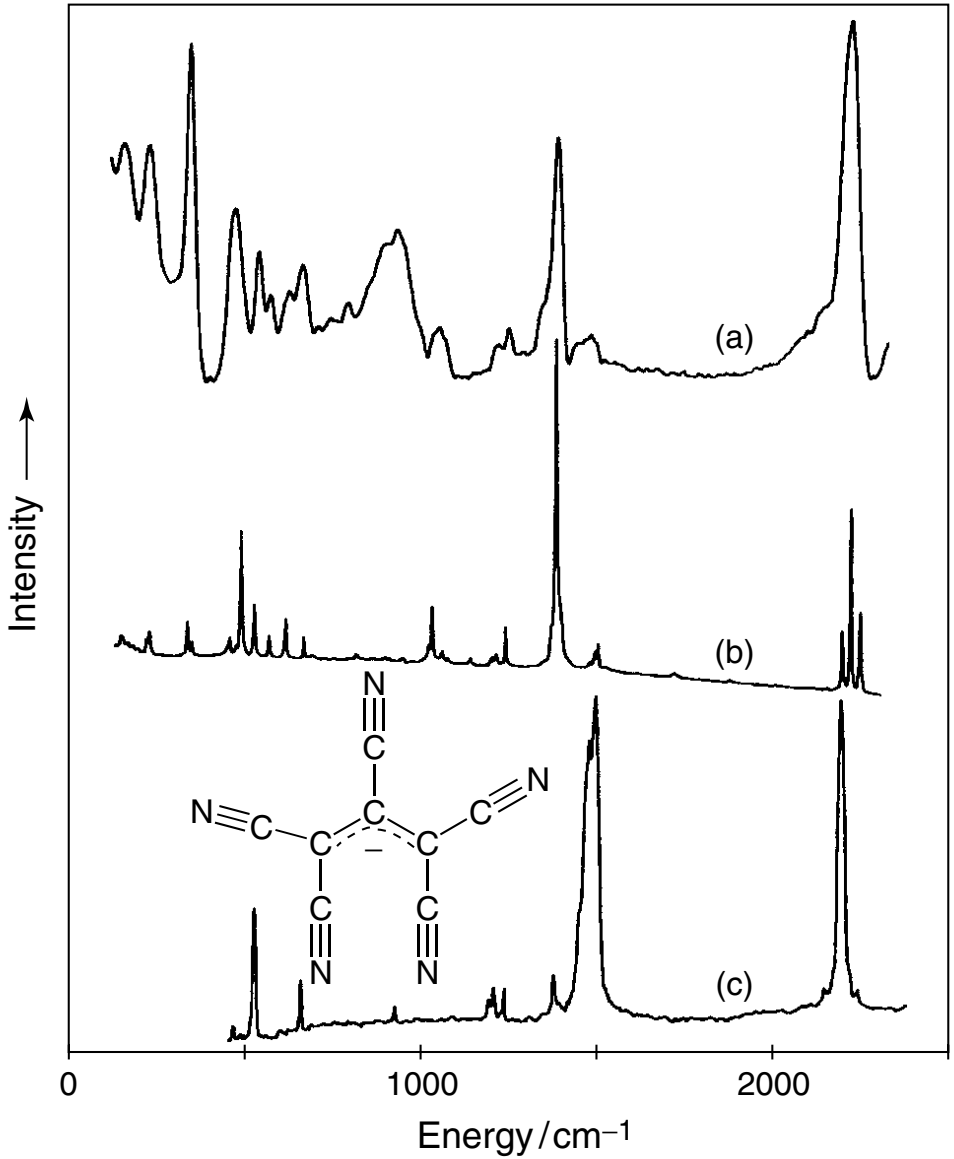

Figure 9. (a) IETS, (b) Raman (powder), and (c) IR (in KBr) spectra obtained from the cesium salt of pentacyanopropenide, CsPCP. [Reproduced by permission of the American Chemical Society from K.W. Hipps and U. Mazur, *J. Phys. Chem.*, **97**, 7803 (1993).]

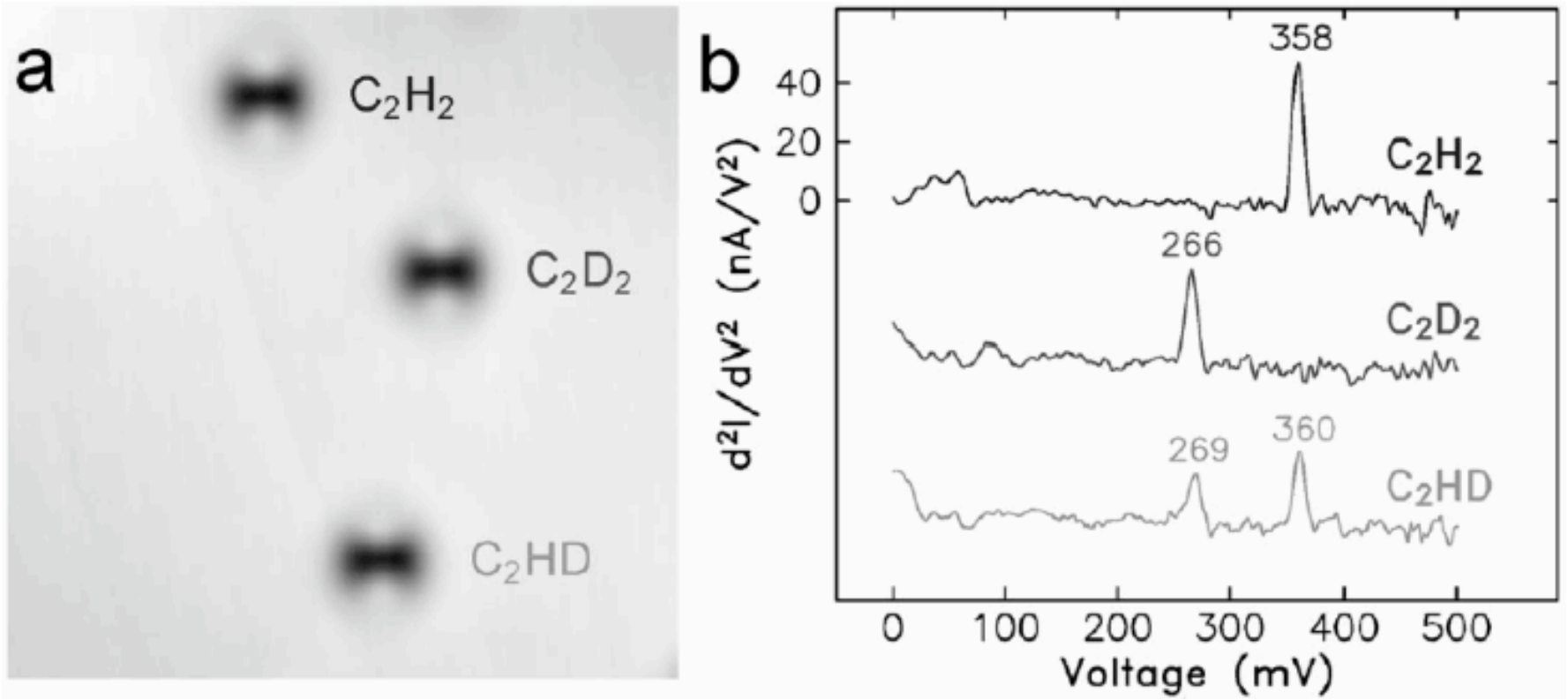

Isotope effect

B.C. Stipe, M.A. Rezaei, and W. Ho, Science 280, 1732 (1998).

56 x 56 Å^2 STM image and STM-IETS spectra of acetylene isotopes on Cu(001), 8 K.

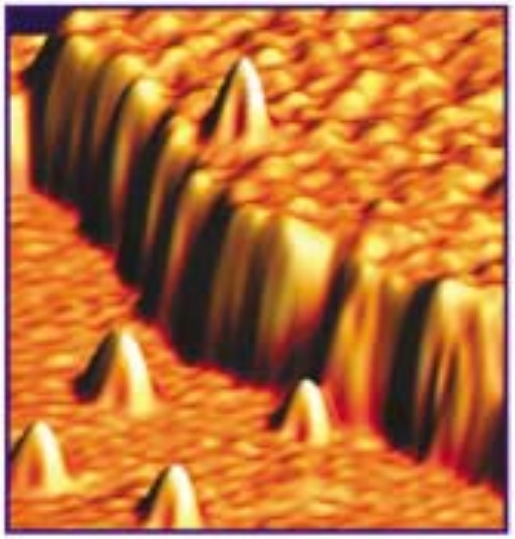

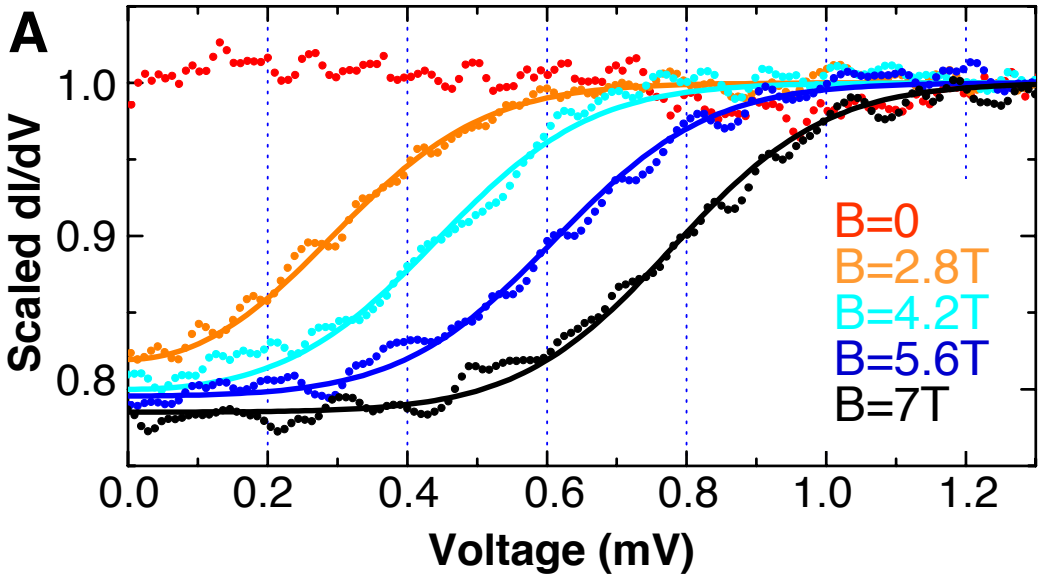

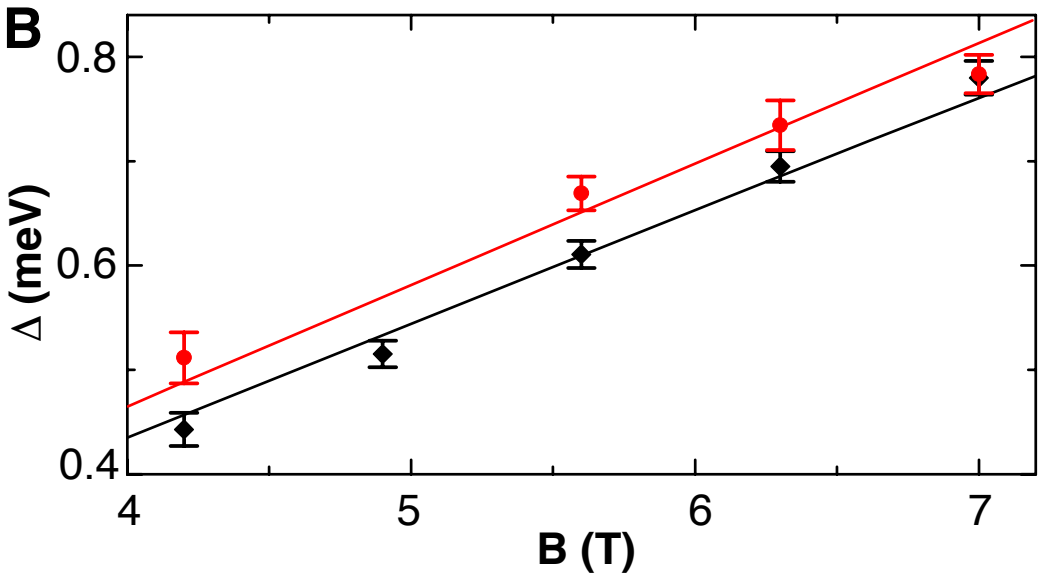

Single-atom spin-flip

A.J. Heinrich, et al. , Science (2004).

Mn atoms on NiAl (partially covered with Al2O3)

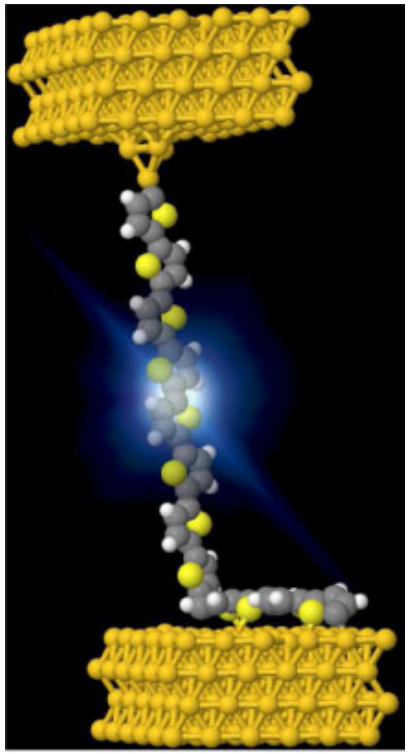

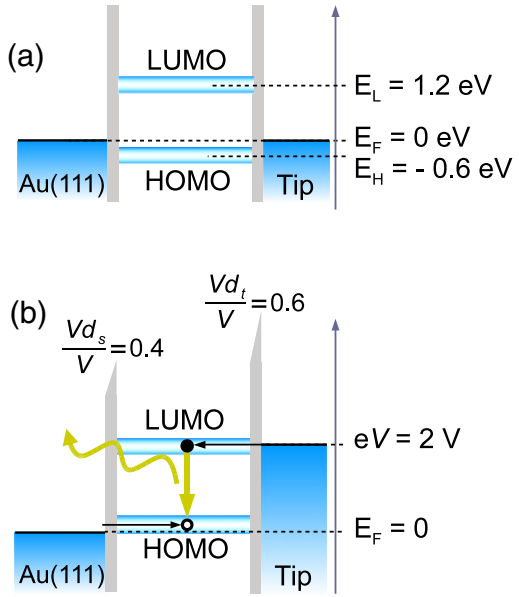

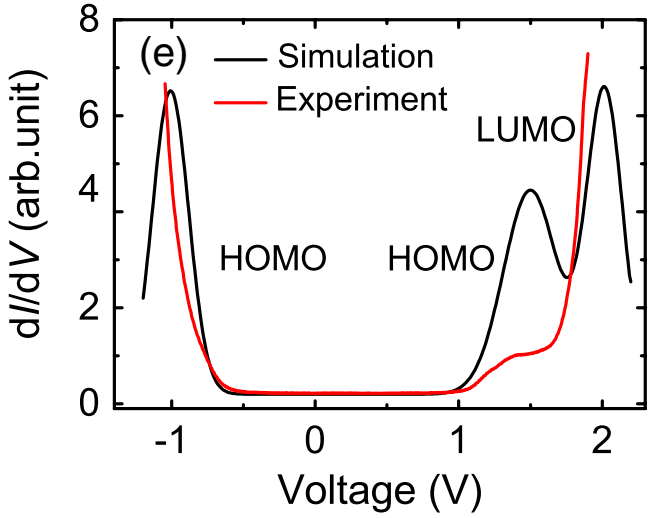

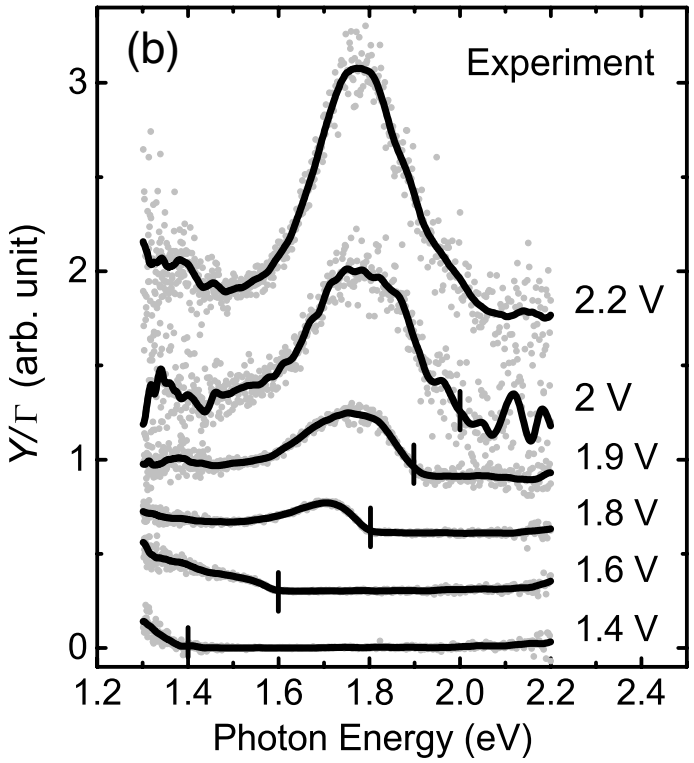

Single-molecule light emitting diode

G. Reecht, et al. , Phys. Rev. Lett. (2014).

Electroluminescence of polythiophene

Photon-assisted tunneling at the atomic scale: Probing resonant Andreev reflections from Yu-Shiba-Rusinov states

Olof Peters,[1] Nils Bogdanoff,[1] Sergio Acero Gonzalez,[2] Larissa Melischek,[2] J. Rika Simon,[1]
Gaël Reecht,[1] Clemens B. Winkelmann,[3] Felix von Oppen,[2] and Katharina J. Franke[1]

[1] *Fachbereich Physik, Freie Universität Berlin, 14195 Berlin, Germany*
[2] *Dahlem Center for Complex Quantum Systems and Fachbereich Physik, Freie Universität Berlin, 14195 Berlin, Germany*
[3] *Université Grenoble Alpes, CNRS, Institut Neél, 25 Avenue des Martyrs, 38042 Grenoble, France*

(Dated: January 28, 2020)

Microwave-driven tunneling processes

O. Peters, et al., arXiv (2020).

Tien-Gordon model

T=1.6 K
V_{ac}*= 20 μV*

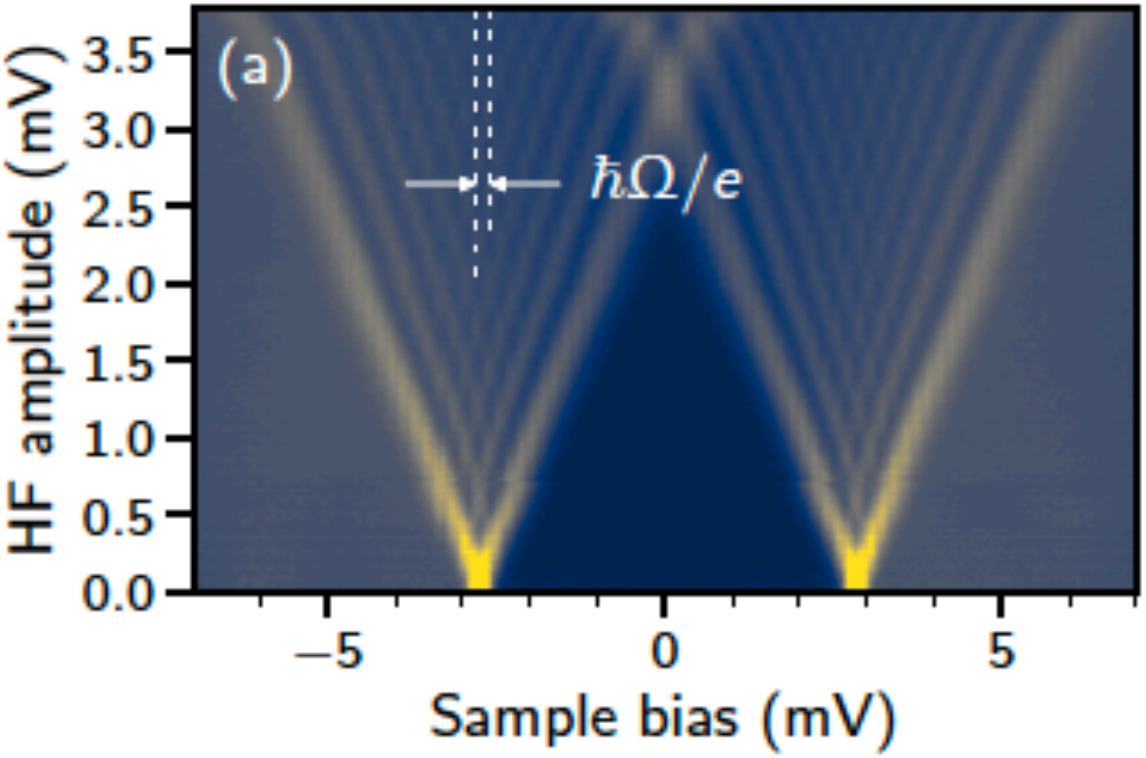

The Abrikosov vortex lattice

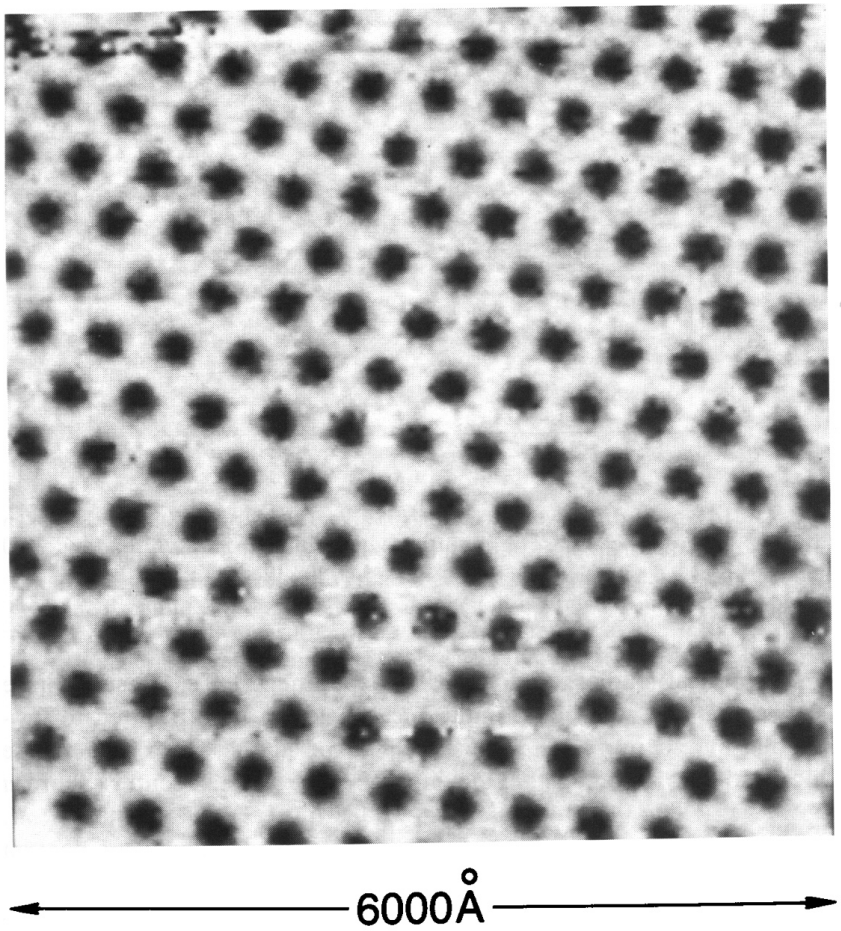

Fig. 4.120. Abrikosov flux lattice produced by 1 T magnetic field in $NbSe_2$ at 1.8 K. The gray scale corresponds to d*I*/d*U* (Hess *et al.*, 1989).

H.F. Hess et al.,
Phys. Rev. Lett. 62, 214 (1989).

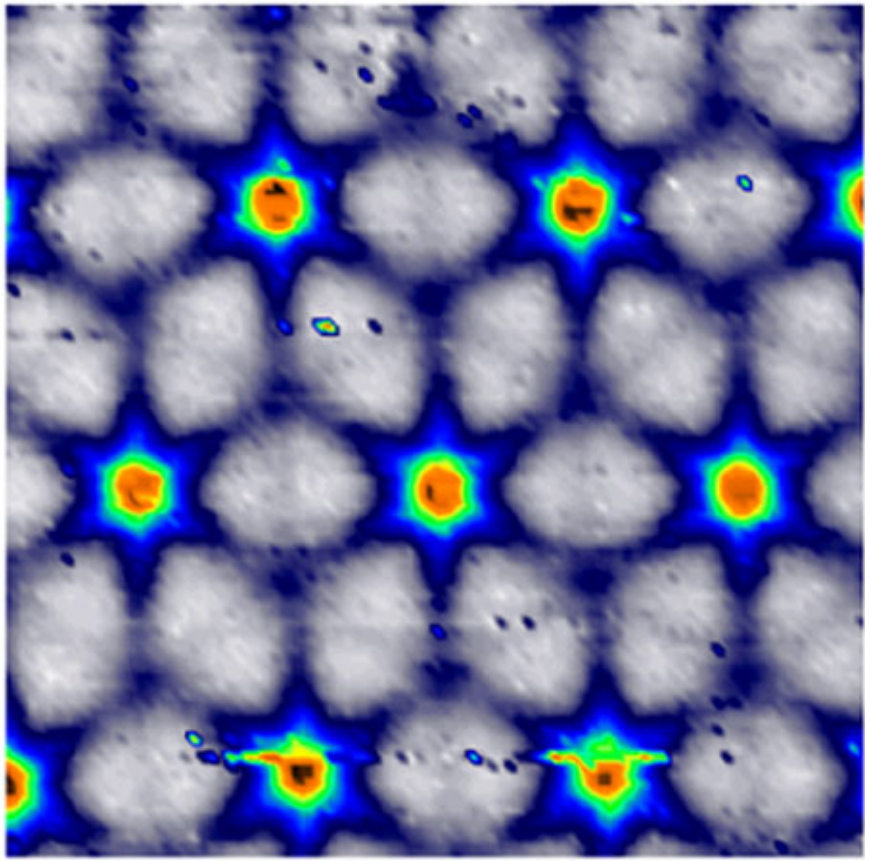

360 x 360 nm^2, 0.1 K, 0.15 T

I. Guillamon, H. Suderow et al.,
Phys. Rev. Lett. 101, 166407 (2008).

Yu-Shiba-Rusinov bound states

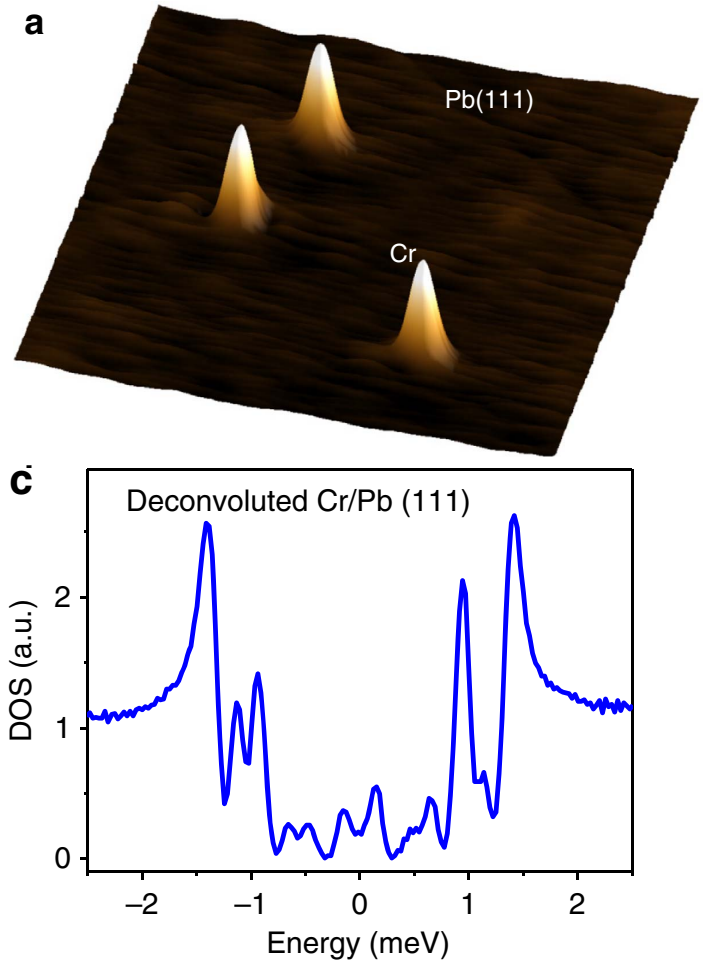

D-J Choi et al.,
Nature Comm. 8, 15175 (2017).

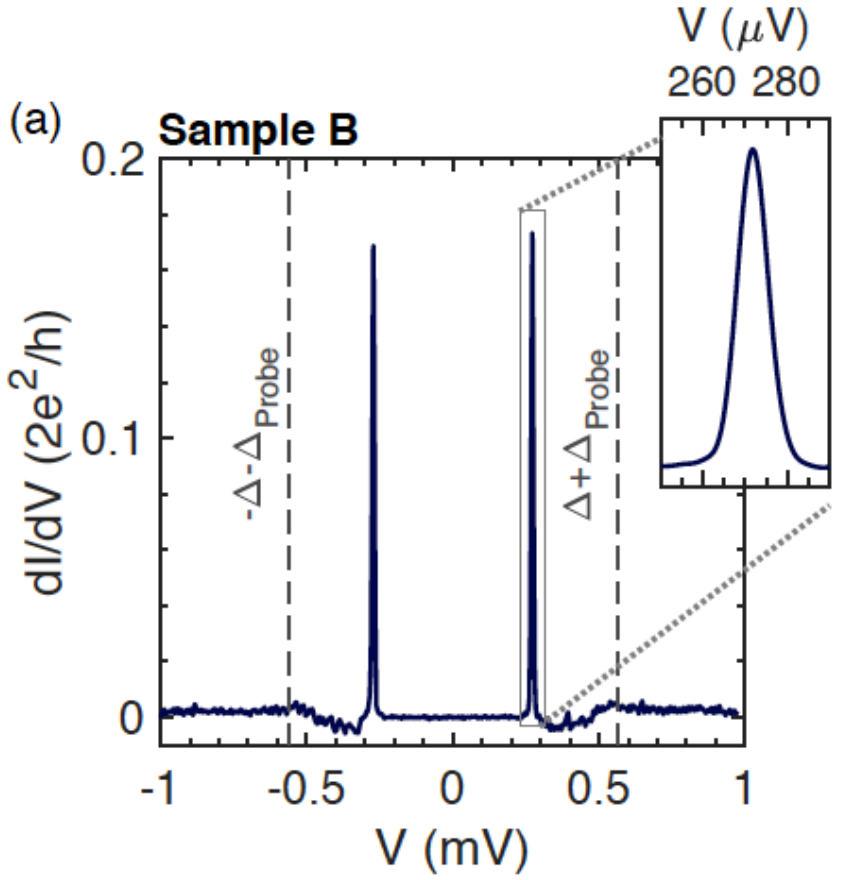

Magnetic impurity on a superconducting Al lead (T=80 mK).

A. Garcia Corral, C.B. Winkelmann et al. arXiv:1912.04084 (2019).

Yu-Shiba-Rusinov bound states

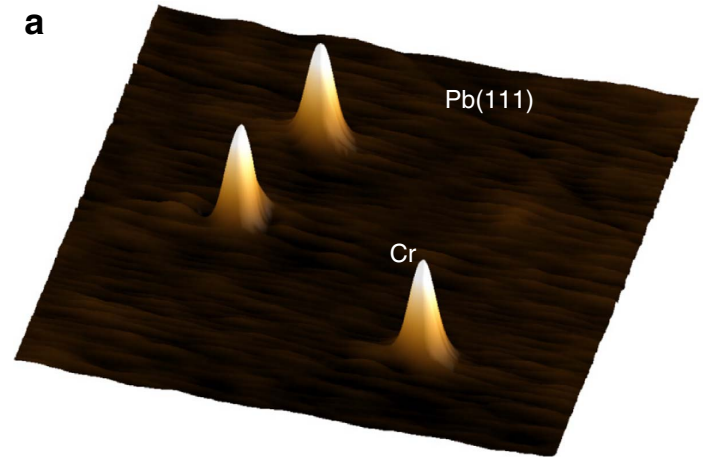

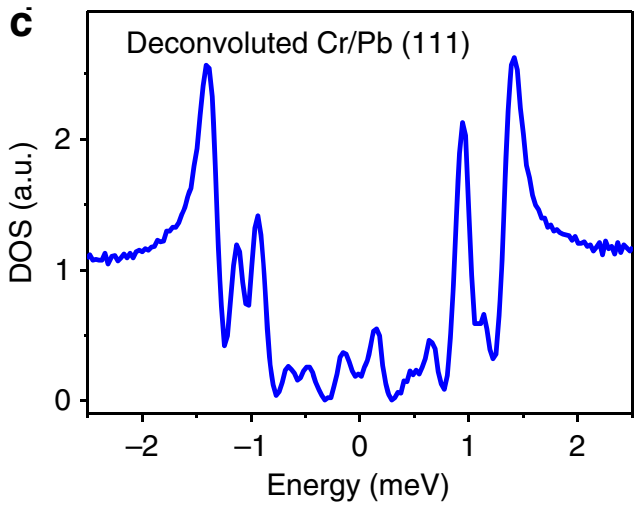

D-J Choi et al.,
Nature Comm. 8, 15175 (2017).

O. Peters, C.B. Winkelmann, K. Franke et al.,
unpublished

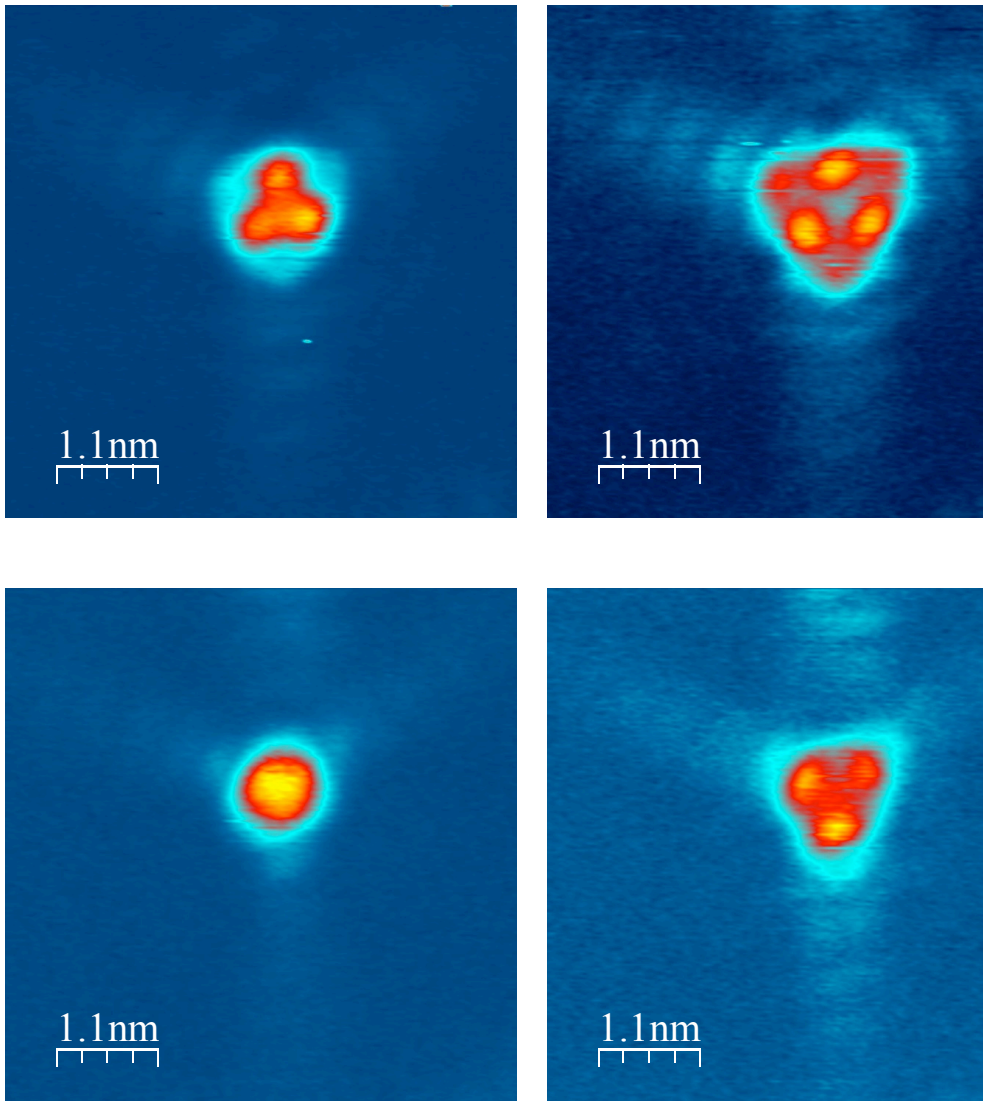

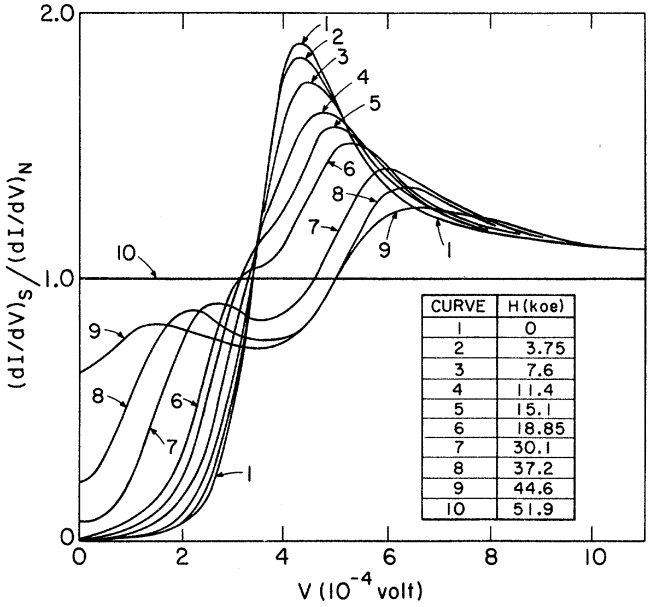

FIG. 1. Experimental plots for several values of magnetic field of the superconducting conductance $(dI/dV)_s$ divided by the normal-state conductance $(dI/dV)_n$.

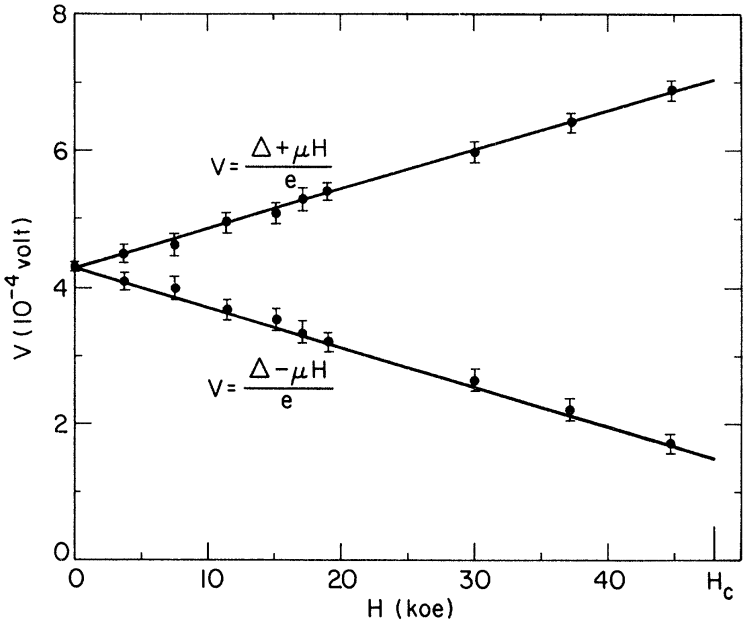

FIG. 2. Voltage corresponding to the maxima of the spin-up and spin-down density-of-states curves determined from Fig. 1 by the graphical method illustrated in Fig. 3. The lines represent the theoretically expected result that $eV=(\epsilon^2+\Delta^2)^{1/2}\pm\mu H$.

Meservey and Tedorow,
Phys. Rev. Lett. (1970)

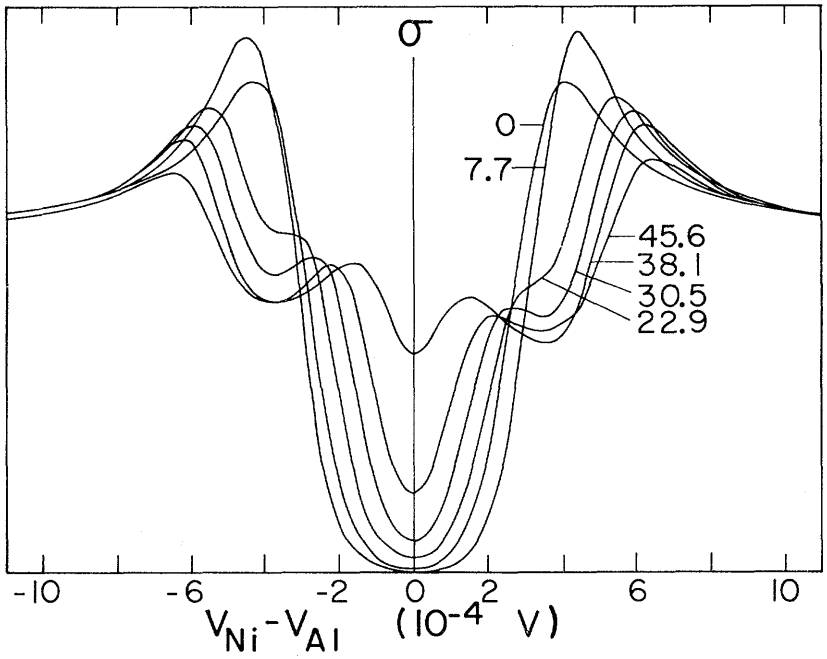

FIG. 7. Measured conductance vs voltage for an $Al-Al_2O_3-Ni$ tunnel junction for several values of the magnetic field H (kOe).

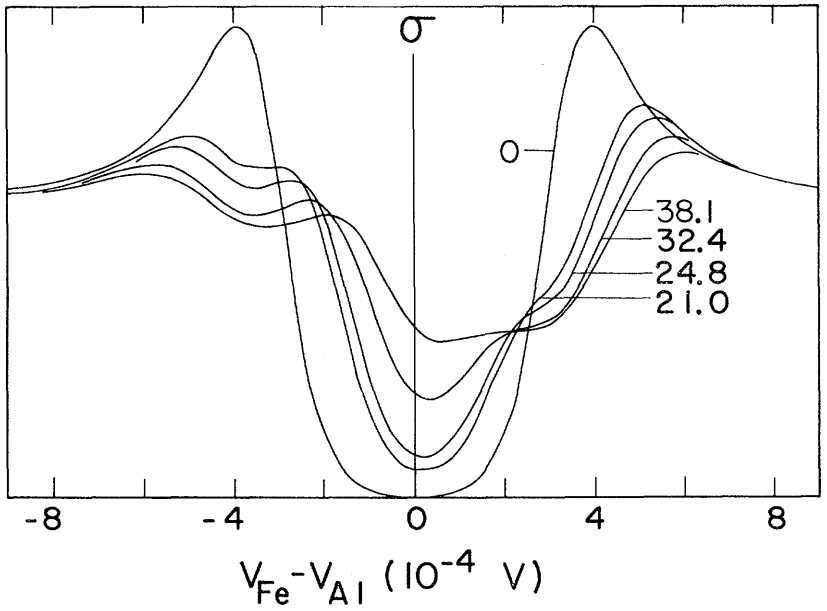

FIG. 9. Measured conductance vs voltage for a typical $Al-Al_2O_3-Fe$ junction at several values of magnetic field H (kOe).

Tederow and Meservey,
Phys. Rev. B (1973)

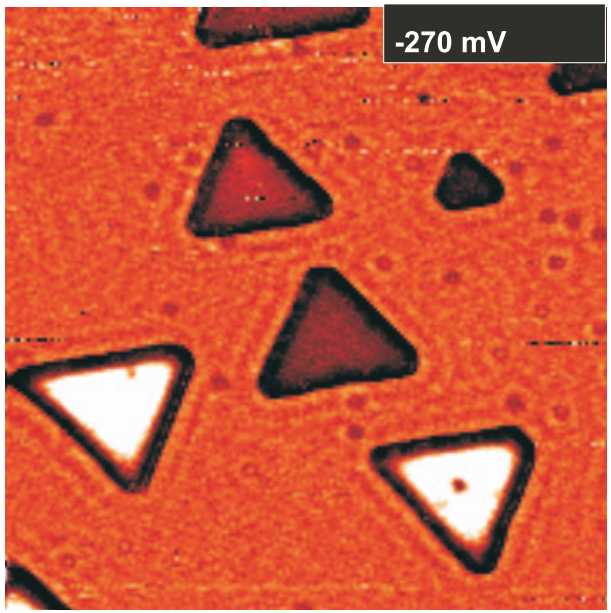

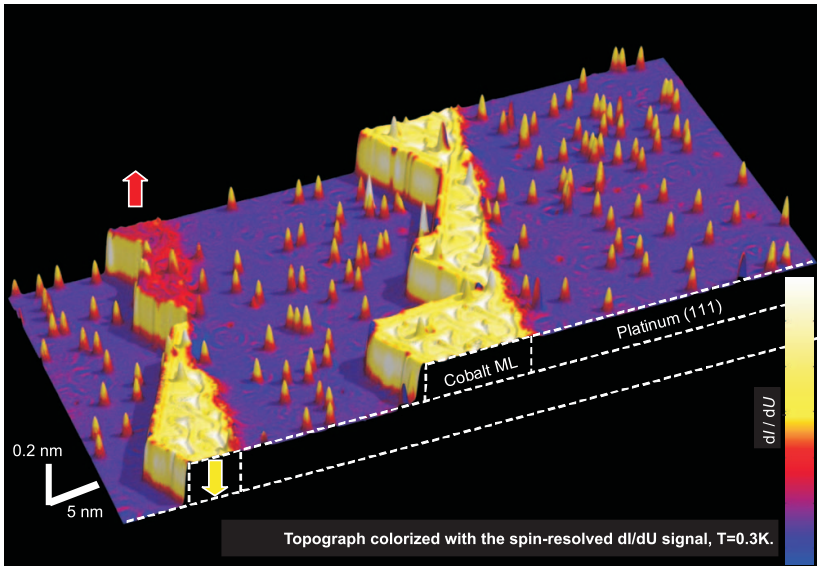

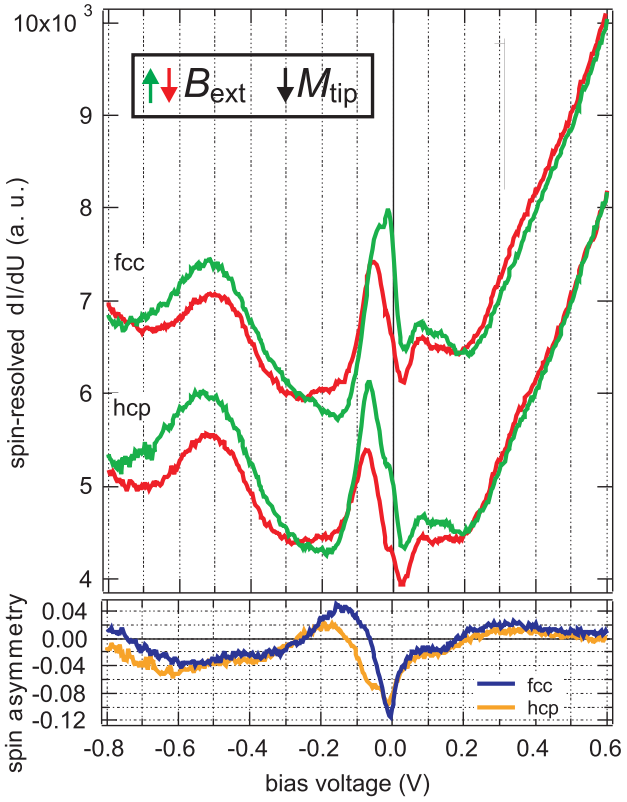

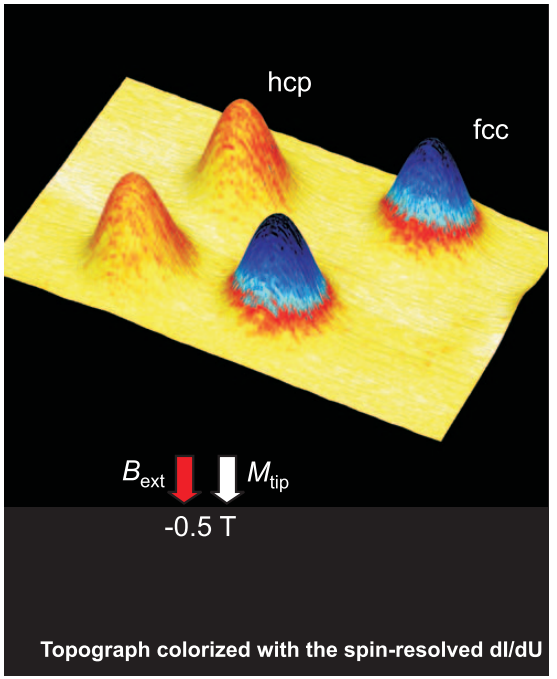

Pietzsch et al.,
Phys. Rev. Lett. (2004)

Meier et al.,
Science (2008)

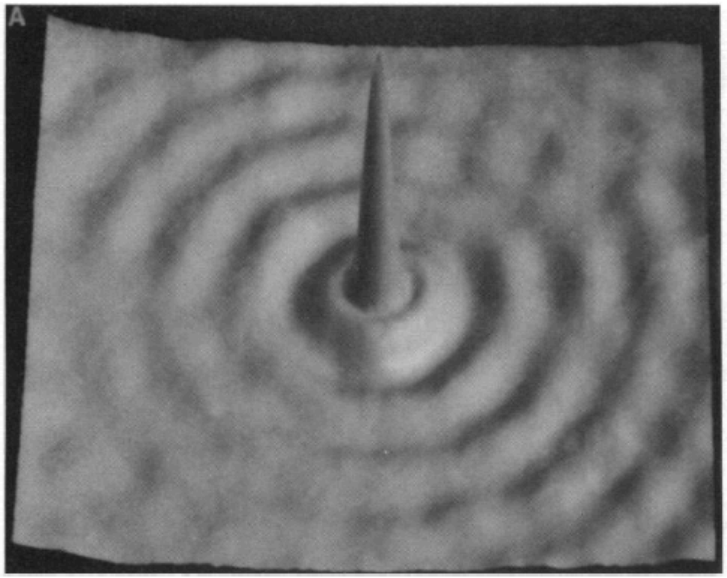

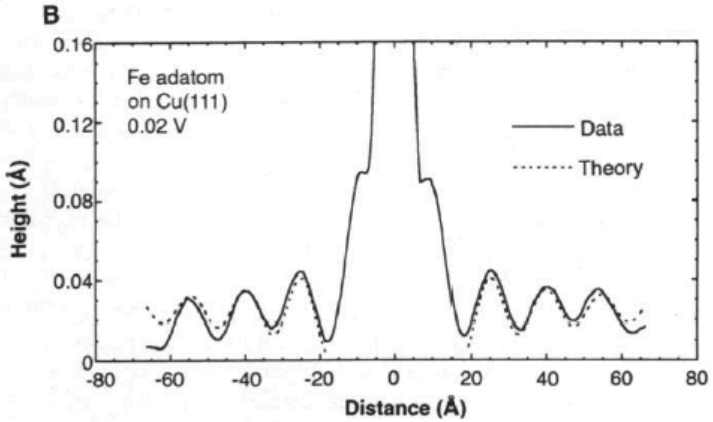

Fig. 1. (**A**) Constant current 130 Å × 130 Å image of an Fe adatom on the Cu(111) surface (V = 0.02 volt, I = 1.0 nA). The apparent height of the adatom is ~0.9 Å. The concentric rings surrounding the Fe adatom are standing waves due to the scattering of surface state electrons with the Fe adatom. (**B**) Solid line: average of three cross sections taken through the center of the Fe adatom image in (A). Dashed line: fit of Eq. 1 to the cross section (the data was fit only up to 18 Å from the center of the adatom).

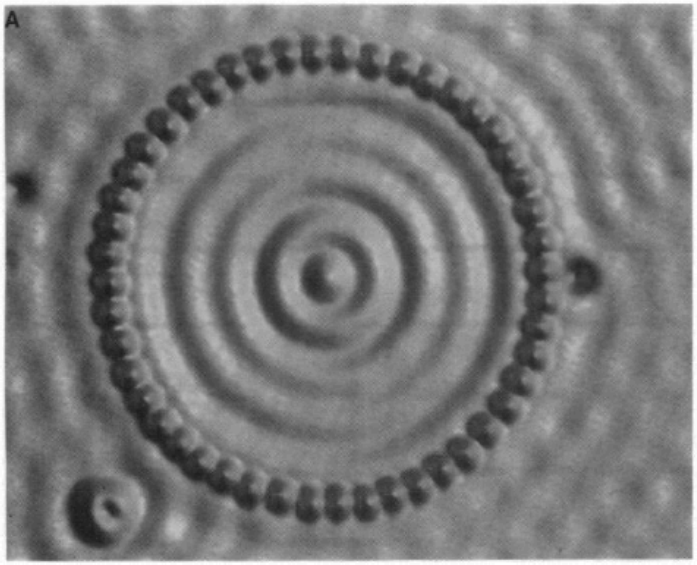

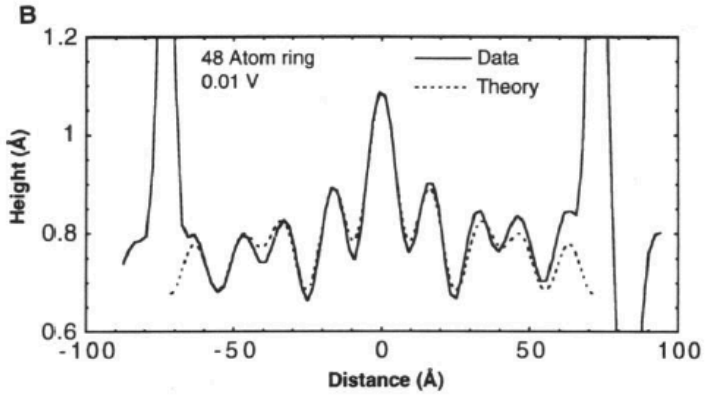

Crommie et al., Science (1993)

Fig. 2. Spatial image of the eigenstates of a quantum corral. (**A**) 48-atom Fe ring constructed on the Cu(111) surface (V = 0.01 volt, I = 1.0 nA). Average diameter of ring (atom center to atom center) is 142.6 Å. The ring encloses a defect-free region of the surface. (**B**) Solid line: cross section of the above data. Dashed line: fit to cross section using a linear combination of $|5,0\rangle$, $|4,2\rangle$, and $|2,7\rangle$ eigenstate densities.

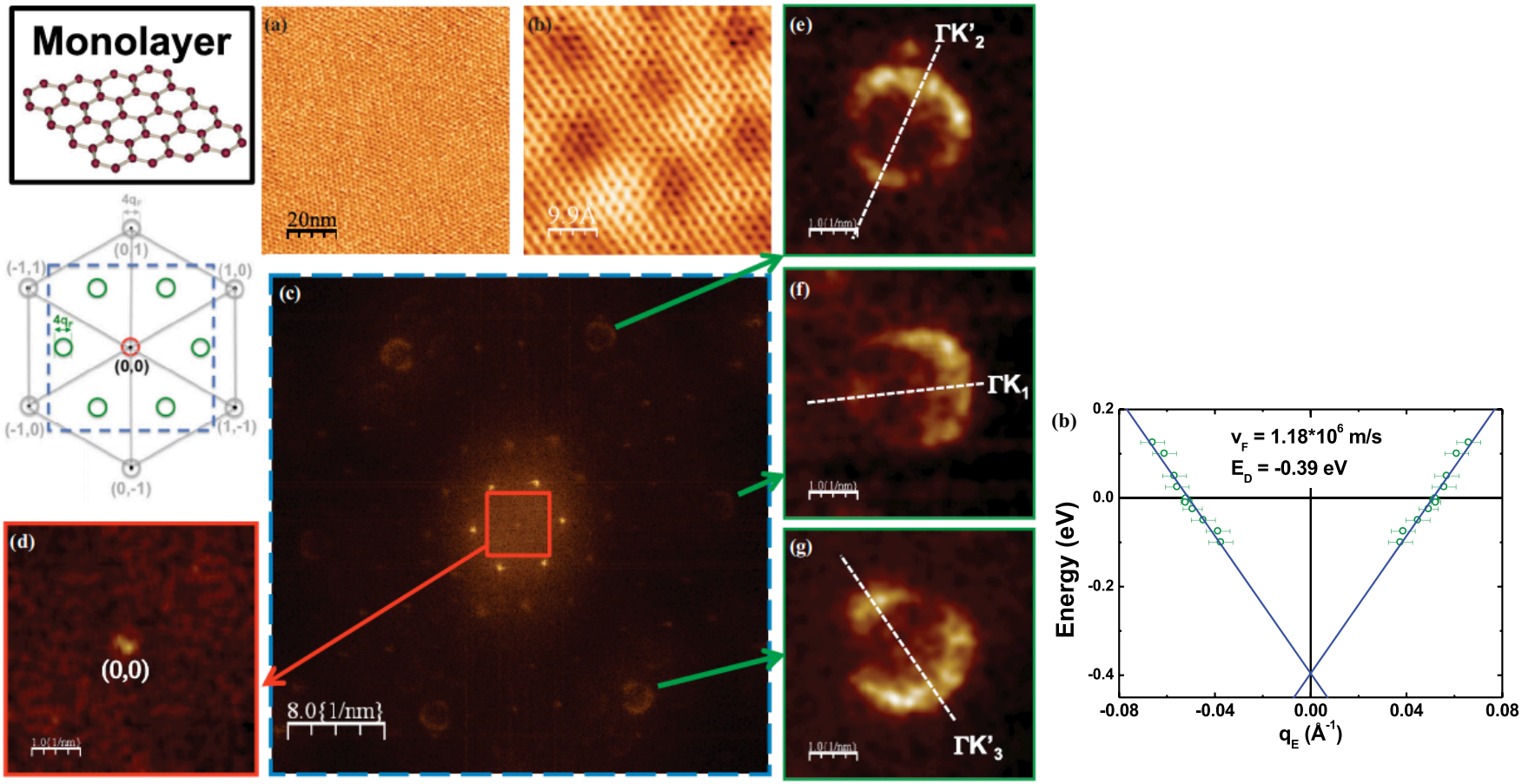

FIG. 2. (Color online) (a) A 100 × 100 nm^2 constant-current STM image on ML graphene on SiC(0001). Sample bias: −4 mV. Number of pixels: 2048 × 2048. (b) A 5 × 5 nm^2 numerical zoom of (a), showing a hexagonal atomic pattern of period 0.24 nm characteristics of the graphene's honeycomb structure. A long-range periodic superstructure (period 1.9 nm) is also present, inferred to the interface with the buffer layer (see text). (c) Two-dimensional fast Fourier transform (2D FFT) of (a). Image size: 40 × 40 nm^{-2}. (d) Central area of (c) showing the absence of intensity ring with radius $2q_F$. (e)–(g) Zoom-in on the three $2q_F$ outer rings in (c) indicated by arrows. Image sizes are 5 × 5 nm^{-2} for (d)–(g).

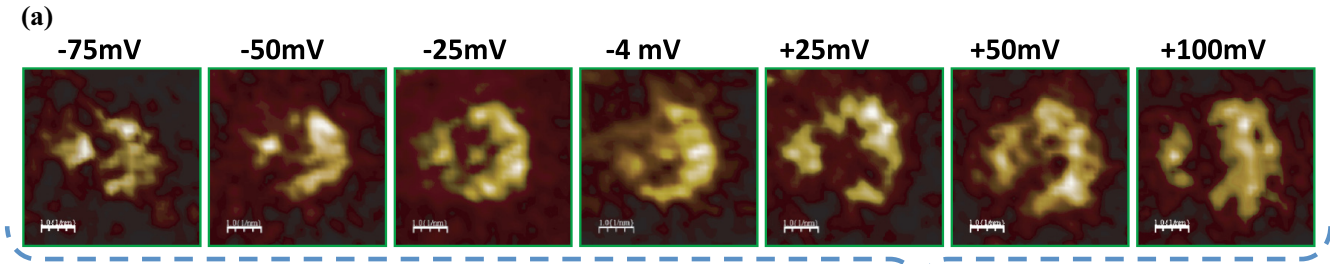

Mallet et al.,
Phys. Rev. B (2012)

Fourier-transform STM

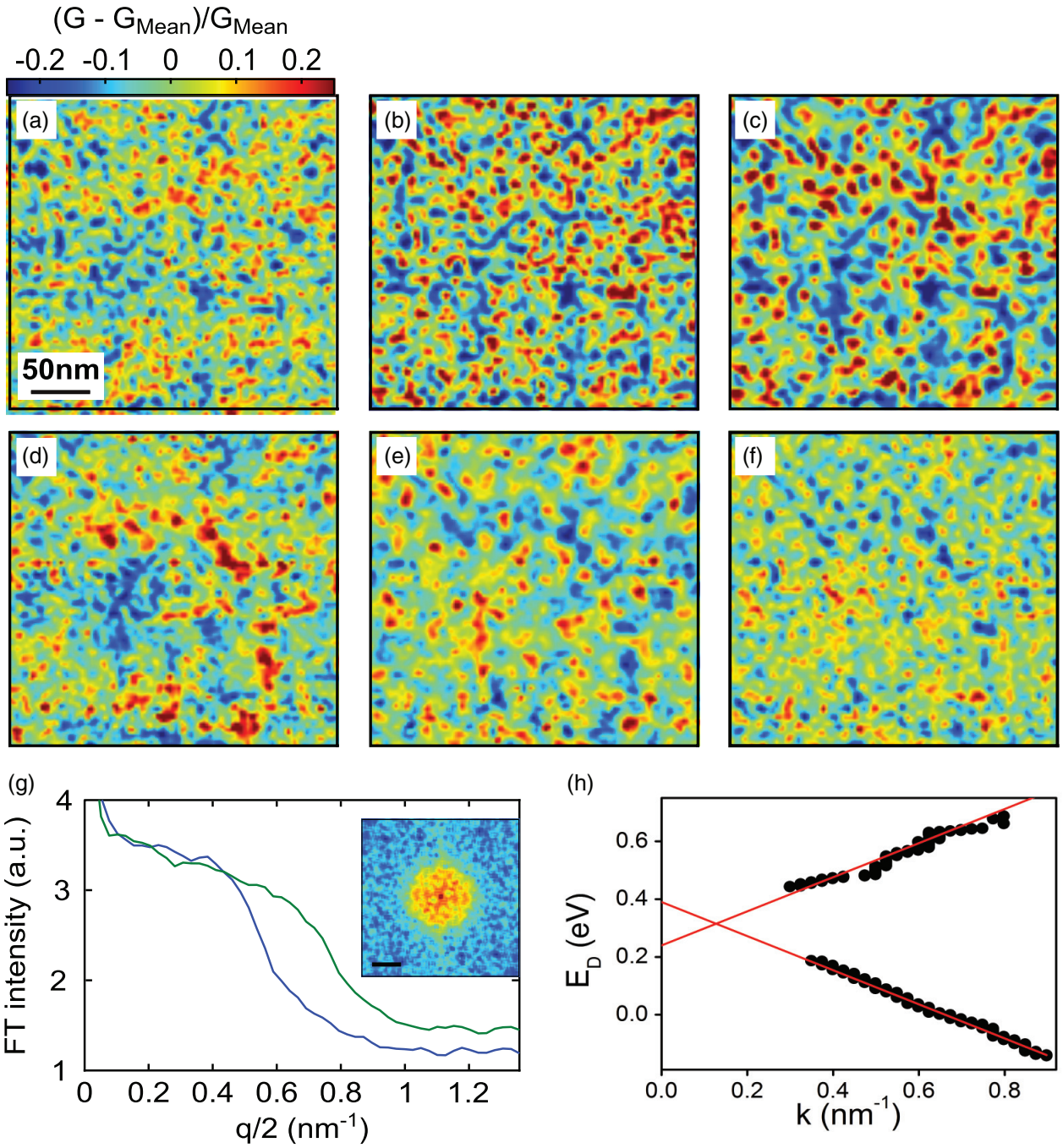

Martin et al.,
Phys. Rev. B (2015)